Nine-vertex Polyhedral Iridamonocarbaborane Chemistry. Products of Thermolysis of $[(CO)(PPh_3)_2IrCB_7H_8]$ and Emerging Alternative Cluster-geometry Patterns†

Bohumil Štíbr,[a] **John D. Kennedy,**[b] **Eva Drdáková**[a] **and Mark Thornton-Pett**[b]
[a] *Institute of Inorganic Chemistry, Academy of Sciences of the Czech Republic, 25068 Řež near Prague, The Czech Republic*
[b] *School of Chemistry, The University of Leeds, Leeds LS2 9JT, UK*

Thermolysis of $[7\text{-}(CO)\text{-}7,7\text{-}(PPh_3)_2\text{-}7,1\text{-}IrCB_7H_8]$ **1** at 250 °C resulted in isomerisation to give orange air-stable $[7\text{-}(CO)\text{-}7\text{-}H\text{-}7,9\text{-}(PPh_3)_2\text{-}7,1\text{-}IrCB_7H_7]$ **2** and its 6-(PPh_3) isomer **3** as the major products. The compounds were characterised by NMR spectroscopy and single-crystal X-ray diffraction analysis on **1** and **3**. The CH_2Cl_2 disolvate of **1** is monoclinic, space group $P2_1/n$, with a = 1394.33(10), b = 1276.81(13), c = 2393.5(2) pm, β = 94.163(9)°, and Z = 4, and the structure was refined to $R(R_g)$ = 0.0351(0.0384) for 5991 reflections with $I > 2.0\sigma(I)$. The CH_2Cl_2 monosolvate of **3** is triclinic, space group $P\bar{1}$, with a = 1150.39(11), b = 1177.08(13), c = 1498.3(2) pm, α = 88.192(9), β = 89.506(8), γ = 80.720(9)°, and Z = 2, and the structure was refined to $R(R_g)$ = 0.0299(0.0311) for 5864 reflections with $I > 2.0\sigma(I)$. The nine-vertex $\{IrCB_7\}$ cluster structures of **1** and **3** have quadrilateral open faces (B–B *ca.* 220 pm) and therefore '*isonido*' geometries although of formal *closo* constitution. The cluster opening is briefly discussed in the context of a nine-vertex *closo–isonido–isocloso* structural continuum, in the context of other contemporaneously recognised structural continua in twelve-, eleven-, ten- and eight-vertex boron cluster chemistry, and thence in the context of emerging general structural patterns that interrelate the *isocloso*, *isonido* and *isoarachno* cluster geometries.

We have become interested in formally *closo* nine-vertex heteroboranes of ostensibly closed tricapped trigonal-prismatic geometry **I**, and in the recognition that many of these exhibit partial opening towards the square-faced *isonido* geometry **II**. Recently we have reported on the iridamonocarbaborane $[7\text{-}(CO)\text{-}7,7\text{-}(PPh_3)_2\text{-}7,1\text{-}IrCB_7H_8]$ **1** which exhibits such an open geometry (schematic **III**).[1] We surmised that further examples of this interesting structural type would be formed by thermolytic isomerisation of **1**, and here report some experimental results in this area. The numbering system used is for the nine-vertex *closo* structure **IV**.

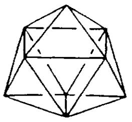

I

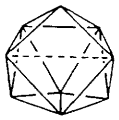

II

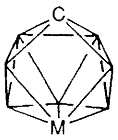

III

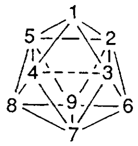

IV

Results and Discussion

Thermolysis of a sample of $[7\text{-}(CO)\text{-}7,7\text{-}(PPh_3)_2\text{-}7,1\text{-}IrCB_7H_8]$ **1** at 25 °C (reaction scale *ca.* 13 μmol) followed by chromatographic separation of the products yielded the starting substrate **1** (10% recovery) together with yellow products **2** and **3** (yields 26 and 48% respectively, based on the amount of compound **1** consumed). NMR spectroscopy (Table 1 and Fig. 1) indicated that compounds **2** and **3** had the same molecular formulae and similar cluster configurations to those of **1**, and that the thermolysis had resulted in exchange of boron-bound hydride with iridium-bound triphenylphosphine groups to give two isomers of formulation $[7\text{-}(CO)\text{-}7\text{-}H\text{-}7\text{-}(PPh_3)\text{-}7,1\text{-}IrCB_7H_7(PPh_3)]$.

More detailed consideration of the comparative NMR properties, in particular the presumption of low-field $\delta(^{11}B)$ values for metal-adjacent boron positions of lower connectivities, and the shift of $\delta(^{11}B)$ values of some 10–20 ppm to higher field upon substitution of H by PPh_3, gave the 9- and 6-(PPh_3) configurations **V** and **VI** respectively for **2** and **3**. These are therefore formulated as $[7\text{-}(CO)\text{-}7\text{-}H\text{-}7,9\text{-}(PPh_3)_2\text{-}7,1\text{-}IrCB_7H_7]$ and $[7\text{-}(CO)\text{-}7\text{-}H\text{-}6,7\text{-}(PPh_3)_2\text{-}7,1\text{-}IrCB_7H_7]$ respectively. The small deviations in $\delta(^{11}B)$ from the 2:2:2:1 relative-intensity pattern otherwise expected for a symmetrical cluster **V** in compound **2** arise from differential *trans* effects arising from the asymmetric exopolyhedral $\{Ir(CO)H(PPh_3)\}$ ligand sphere. Trace amounts of an additional product **4** were evident from the NMR spectra of some preliminary samples of compound **2** (see footnote *c* in Table 1). It seems probable that compound **4** is one of the remaining isomers, either the 2- or the 3-(PPh_3) species (schematic cluster structures **VII** and **VIII**), most likely the 2 isomer (structure **VII**) which has the PPh_3 substituent on a boron site adjacent to the metal in common with the other products **2** and **3**.

Another species **5** observed during the course of these experiments should also be noted. In the early stages of the work two *ca.* 1 mg samples of starting material **1** that had been purified by HPLC were observed by NMR spectroscopy in $CDCl_3$ solution readily to undergo quantitative change ($t_{\frac{1}{2}}$ *ca.*

---

† *Supplementary data available:* see Instructions for Authors, *J. Chem. Soc., Dalton Trans.*, 1994, Issue 1, pp. xxiii–xxviii.

Table 1 Measured NMR data for [(CO)(PPh$_3$)$_2$IrCB$_7$H$_8$] **1** [H(CO)(PPh$_3$)IrCB$_7$H$_7$(PPh$_3$-9)] **2**, [H(CO)(PPh$_3$)IrCB$_7$H$_7$(PPh$_3$-6)] **3** and the unknown compound **5**, in CDCl$_3$ solution at 294–297 K

Tentative assignment	**1**[a]		**2**[b,c]		**3**[d]		**5**[e]	
	δ(^{11}B)	δ(^{1}H)	δ(^{11}B)	δ(^{1}H)	δ(^{11}B)	δ(^{1}H)	δ(^{11}B)	δ(^{1}H)
6,8	+32.3[f]	+5.91[f]	+24.2 +20.8	+6.08 +6.06	+37.7 +13.0	+6.51[g] —[h]	+29.1[f]	+6.16[f]
3,4	−0.5[f]	+3.25[f]	−7.9 −10.1	+2.89 +2.89	−1.7 −7.6	+3.08[i] +3.06[i]	+0.9[f]	+3.51[f]
2,5	−18.8[f]	+1.66[f]	−16.5 −17.0	+1.59 +1.81	−17.0 −20.0	+2.17[i] +1.78[i]	−19.9[f]	+1.96[f]
9	−27.2	−0.84	−37.9	—[j]	−31.0	−1.20	−27.0	−0.89
{CH}	—	+2.34	—	+2.24	—	+2.72	—	+2.52
{IrH}	—	—	—	−14.41[k]	—	−8.75[l]	—	—

[a] δ(^{31}P) +4.7 (sharp); see also ref. 1. [b] δ(^{31}P) +10.9 (sharp) and +4.2 (br). [c] Some samples contained small quantities of a second compound **4** with δ(^{11}B) *ca.* +33, +27, +1, −5 and −36 (others hidden), δ(^{1}H)(CH) +1.94, and δ(^{31}P) +9.5 (sharp) and +41.9 (br). [d] δ(^{31}P) +20.4 (sharp) and +20.1 (br q, splitting *ca.* 180 Hz). [e] δ(^{31}P) +29.3 (sharp). [f] Relative intensity 2 BH. [g] Doublet splitting *ca.* 23 Hz [^{n}J(^{31}P–^{1}H) ?]. [h] P-Substituted; doublet splitting ^{1}J(^{31}P–^{11}B) 173 Hz. [i] [^{1}H–^{1}H] correlation spectroscopy gave cross-peaks between these resonances and that at δ(^{1}H) +2.72 (CH). [j] P-Substituted; doublet splitting ^{1}J(^{31}P–^{11}B) *ca.* 120 Hz. [k] Doublet splitting ^{2}J(^{31}P–^{1}H) 21.5 Hz. [l] Apparent 1:2:1 triplet structure, repeated splitting *ca.* 19.5 Hz.

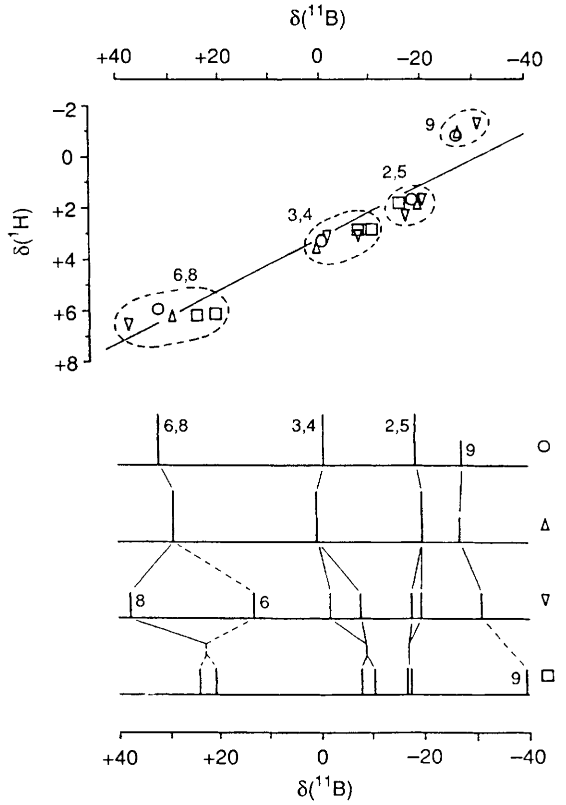

Fig. 1 Selected NMR data for compounds **1** (○), **2** (□), **3** (▽) and **5** (△). The bottom set of diagrams are stick representations of the chemical shifts and relative intensities in the ^{11}B spectra, with lines joining equivalent positions in the four compounds. Hatched lines join the P-substituted positions for compounds **2** and **3**. The top diagram plots δ(^{1}H) *versus* δ(^{11}B) for the {BH} units in the four compounds. The line drawn has slope δ(^{11}B):δ(^{1}H) 10:1, intercept +3.20 in δ(^{1}H)

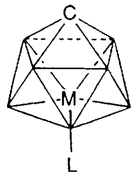

V

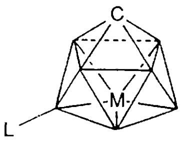

VI

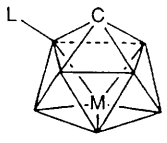

VII

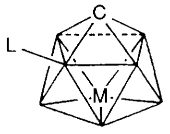

VIII

1 d at 294 K, 3.2 mmol dm^{-3} solution) to a species **5**. The latter had very similar ^{11}B and ^{1}H NMR properties to those of compound **1**, but differed considerably in δ(^{31}P) (Table 1). Interestingly, however, larger pure samples of compound **1** that we prepared subsequently in order to examine the conversion of **1** into **5**, and thence to examine the precise nature of compound **5**, have exhibited no change (currently we have a *ca.* 17 mmol dm^{-3} sample of **1** in CDCl$_3$ which exhibits no trace of **5** after 20 months at *ca.* 290 K). This phenomenon is of interest, but all we can do at present is to note that, because of the particular collaborative nature of our joint work, the starting materials, precursors, and solvents may well have come from different combinations of sources in each case.

We have confirmed the constitution of [7-(CO)-7-H-6,7-(PPh$_3$)$_2$-7,1-IrCB$_7$H$_7$] **3** by single-crystal X-ray diffraction analysis. Crystals were obtained from a dichloromethane–hexane mixture to give a dichloromethane monosolvate. Selected interatomic distances and angles are in Tables 2 and 3, and fractional atomic coordinates are in Table 7. The molecular structure (Fig. 2) is seen to be based on the classical *closo* tricapped trigonal-prismatic shape (structure **I**) that would be predicted by the Williams–Wade[3,4] formalism. However, as observed for compound **1**,[1] there is a marked opening of the Ir(7)B(3)B(4)C(1) 'diamond' to give a quadrilateral open face (structure **II**), with an essentially non-bonding interboron distance of 218.7(9) pm. The {IrH(CO)(PPh$_3$)} orientation is such that the B(PPh$_3$) and Ir(PPh$_3$) groups are mutually transoid, although it is not clear whether this is the result of steric or electronic control.

As part of this work we also have isolated a crystalline 1:2 CH$_2$Cl$_2$ disolvate of compound **1**, [7-(CO)-7,7-(PPh$_3$)$_2$-7,1-IrCB$_7$H$_8$]·2CH$_2$Cl$_2$, which permitted the examination by single-crystal X-ray diffraction analysis of the effect of a different lattice environment on the interesting open-faced nature of this species, the previously reported structure of **1** having been obtained for an unsolvated crystal.[1] The crystals were grown from a dichloromethane solution of **1** that had been overlayered by an equivalent volume of hexane. A drawing of the molecular structure is in Fig. 3, and salient interatomic distances and angles are in Tables 4 and 5. Fractional atomic coordinates are in Table 8.

Table 2 Selected interatomic distances (pm) for [7-(CO)-7-H-6,7-$(PPh_3)_2$-7,1-$IrCB_7H_7$] **3** (CH_2Cl_2 monsolvate) with estimated standard deviations (e.s.d.s) in parentheses

P(1)–Ir(7)	232.5(3)	C(10)–Ir(7)	187.1(8)
H(7)–Ir(7)	146(6)		
B(3)–Ir(7)	237.6(8)	B(4)–Ir(7)	241.1(8)
B(6)–Ir(7)	213.4(8)	B(8)–Ir(7)	214.6(8)
B(9)–Ir(7)	236.0(8)	C(1)–Ir(7)	320.0(6)
C(111)–P(1)	183.8(5)	C(211)–P(2)	180.8(5)
C(121)–P(1)	183.7(5)	C(221)–P(2)	182.6(5)
C(131)–P(1)	182.9(5)	C(231)–P(2)	181.5(5)
O(10)–C(10)	114.0(8)		
B(2)–C(1)	161.3(10)	B(5)–C(1)	163.5(11)
B(3)–C(1)	159.9(10)	B(4)–C(1)	160.2(11)
B(3)–B(2)	178.7(11)	B(4)–B(5)	178.3(12)
B(6)–B(2)	170.9(10)	B(8)–B(5)	170.3(11)
B(9)–B(2)	192.2(10)	B(9)–B(5)	191.6(10)
B(5)–B(2)	189.0(11)		
B(4)–B(3)	218.7(9)		
B(6)–B(3)	172.2(10)	B(8)–B(4)	171.3(11)
B(9)–B(6)	173.1(10)	B(9)–B(8)	176.5(10)
H(1)–C(1)	101(7)	H(9)–B(9)	111(5)
H(2)–B(2)	112(6)	H(5)–B(5)	106(5)
H(3)–B(3)	112(6)	H(4)–B(4)	118(6)
B(6)–P(2)	190.3(8)	H(8)–B(8)	107(5)

Table 3 Selected angles (°) between interatomic vectors for [7-(CO)-7-H-6,7-$(PPh_3)_2$-7,1-$IrCB_7H_7$] **3** (CH_2Cl_2 monosolvate) with e.s.d.s in parentheses

(*i*) At iridium

C(10)–Ir(7)–P(1)	91.5(3)		
H(7)–Ir(7)–P(1)	90.0(23)	H(7)–Ir(7)–C(10)	84.3(23)
B(3)–Ir(7)–P(1)	160.8(2)	B(3)–Ir(7)–C(10)	85.8(3)
B(4)–Ir(7)–P(1)	107.7(3)	B(4)–Ir(7)–C(10)	100.4(4)
B(6)–Ir(7)–P(1)	150.3(2)	B(6)–Ir(7)–C(10)	113.3(3)
B(8)–Ir(7)–P(1)	85.1(3)	B(8)–Ir(7)–C(10)	139.2(3)
B(9)–Ir(7)–P(1)	112.9(2)	B(9)–Ir(7)–C(10)	155.4(2)
B(4)–Ir(7)–B(3)	54.4(3)		
B(6)–Ir(7)–B(3)	44.5(2)	B(8)–Ir(7)–B(4)	43.7(2)
H(7)–Ir(7)–B(3)	109(2)	H(7)–Ir(7)–B(4)	161(2)
B(8)–Ir(7)–B(3)	84.6(3)	B(6)–Ir(7)–B(4)	84.6(3)
B(9)–Ir(7)–B(3)	70.0(3)	B(9)–Ir(7)–B(4)	69.9(3)
H(7)–Ir(7)–B(6)	77(2)	H(7)–Ir(7)–B(8)	136(2)
B(8)–Ir(7)–B(6)	86.1(3)		
B(9)–Ir(7)–B(6)	45.0(2)	B(9)–Ir(7)–B(8)	45.8(2)
H(7)–Ir(7)–B(9)	98(2)		

(*ii*) At carbon and boron

C(1)–B(3)–Ir(7)	105.5(5)	B(2)–B(3)–Ir(7)	99.6(4)
B(2)–B(3)–C(1)	56.6(4)	B(6)–B(3)–Ir(7)	60.3(4)
B(6)–B(3)–C(1)	108.3(5)	B(6)–B(3)–B(2)	58.2(4)
C(1)–B(4)–Ir(7)	103.9(5)	B(5)–B(4)–Ir(7)	98.4(4)
B(5)–B(4)–C(1)	57.5(5)	B(8)–B(4)–Ir(7)	59.9(4)
B(8)–B(4)–C(1)	108.8(6)	B(8)–B(4)–B(5)	58.3(5)
B(3)–C(1)–B(2)	67.6(5)	B(4)–C(1)–B(2)	114.5(6)
B(4)–C(1)–B(3)	86.2(5)	B(5)–C(1)–B(2)	71.2(5)
B(5)–C(1)–B(3)	113.6(5)	B(5)–C(1)–B(4)	66.8(5)

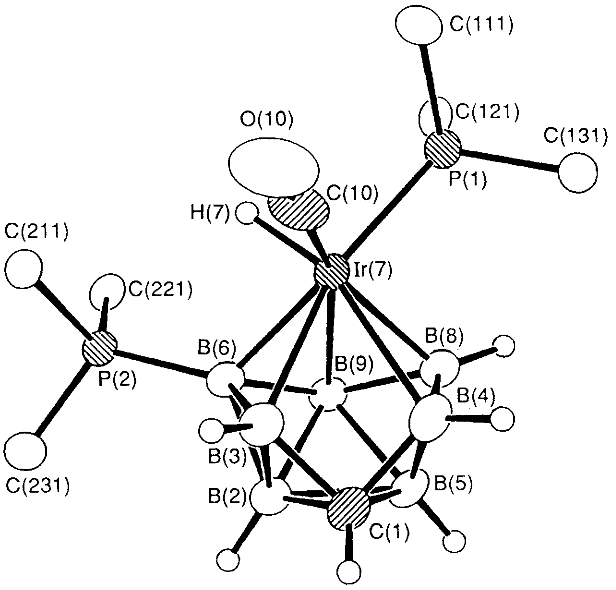

Fig. 2 An ORTEP[2]-type drawing of the crystallographically determined molecular structure of [7-(CO)-7-H-6,7-$(PPh_3)_2$-7,1-$IrCB_7H_7$] **3**

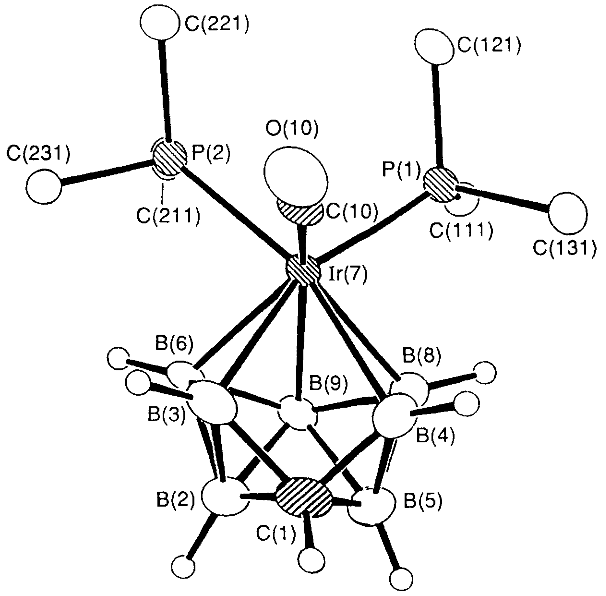

Fig. 3 An ORTEP-type drawing of the crystallographically determined molecular structure of [7-(CO)-7,7-$(PPh_3)_2$-7,1-$IrCB_7H_8$] **1** as determined for its bis(dichloromethane) solvate

The molecular structure is very similar to that found for the non-solvated species, the principal differences being the slight twist in the {$Ir(CO)PPh_3)_2$} bonding sphere relative to the cluster [dihedral angles Ir(7)C(10)C(1)/Ir(7)B(9)C(1) 3.3(3) and 7.3(4)° for the solvated and non-solvated species respectively], and small differences in the Ir–PPh_3 rotamer angles. The Ir(7)B(3)B(4)C(1) quadrilateral open face is again readily apparent, with the degree of opening slightly more marked than in the unsolvated crystals [B(3)–B(4) 226.2(11) and 218.7(9) pm in the solvated and unsolvated species respectively; Ir(7)–C(1) 316.3(7) and 320.0(6) pm respectively].

This quadrilateral face opening in these nine-vertex clusters is reminiscent of a similar opening in *closo* ten-vertex clusters[5] which develops into a *closo–isonido–isocloso* cluster structure continuum as recently described for the {IrB_9} system,[6] and it is of interest to examine the nine-vertex phenomenon in a similar manner. In nine-vertex chemistry (Scheme 1) the *isocloso* structure is that of formal C_{2v} symmetry as in schematic **XI** {exemplified so far only by the species [$(PMe_3)_2HIrB_8H_7Cl$]},[7] and the diamond–square–diamond (d.s.d.)[8] continuum from *closo* (**IX**) through *isonido* (**X**) is characterised by a stretching of the B(3)–B(4) diagonal *b* (numbering as in Figs. 2 and 3), a diminution of the other diagonal *d* (with due allowance for variation in atomic size), and a decrease of the fold angle θ. Many ostensibly *closo* nine-vertex species exhibit B(3)–B(4) stretching,[1] and *b*, *d* and θ values for these[9–14] as well as

Table 4 Selected interatomic distances (pm) for [7-(CO)-7,7-$(PPh_3)_2$-7,1-$IrCB_7H_8$] **1** (CH_2Cl_2 disolvate) with e.s.d.s in parentheses

P(1)–Ir(7)	241.2(3)	P(2)–Ir(7)	241.6(3)
B(3)–Ir(7)	239.8(10)	B(4)–Ir(7)	238.0(9)
B(6)–Ir(7)	219.1(9)	B(8)–Ir(7)	217.4(9)
B(9)–Ir(7)	237.9(9)	C(10)–Ir(7)	188.0(8)
C(111)–P(1)	183.1(5)	C(211)–P(2)	185.2(5)
C(121)–P(1)	184.2(5)	C(221)–P(2)	185.0(5)
C(131)–P(1)	183.9(5)	C(231)–P(2)	184.3(5)
O(10)–C(10)	114.0(8)		
B(2)–C(1)	163.2(13)	B(5)–C(1)	163.7(12)
B(3)–C(1)	160.1(13)	B(4)–C(1)	160.1(12)
B(3)–B(2)	178.2(14)	B(4)–B(5)	177.5(13)
B(6)–B(2)	170.2(12)	B(8)–B(5)	169.1(13)
B(9)–B(2)	191.3(13)	B(9)–B(5)	188.1(13)
B(5)–B(2)	185.1(13)		
B(6)–B(3)	171.0(14)		
B(4)–B(3)	226.2(11)	B(8)–B(4)	171.4(12)
B(9)–B(6)	174.9(12)	B(9)–B(8)	171.6(11)
H(1)–C(1)	102(7)	H(9)–B(9)	107(5)
H(2)–B(2)	120(6)	H(5)–B(5)	104(9)
H(3)–B(3)	118(7)	H(4)–B(4)	113(6)
H(6)–B(6)	107(6)	H(8)–B(8)	117(7)

Table 5 Selected angles (°) between interatomic vectors for [7-(CO)-7,7-$(PPh_3)_2$-7,1-$IrCB_7H_8$] **1** (CH_2Cl_2 disolvate) with e.s.d.s in parentheses

(*i*) At iridium

P(2)–Ir(7)–P(1)	99.0(1)		
C(10)–Ir(7)–P(1)	96.8(3)	C(10)–Ir(7)–P(2)	92.0(3)
B(3)–Ir(7)–P(1)	156.3(2)	B(4)–Ir(7)–P(2)	161.1(2)
B(4)–Ir(7)–P(1)	99.8(3)	B(3)–Ir(7)–P(2)	104.6(3)
B(6)–Ir(7)–P(1)	146.1(2)	B(8)–Ir(7)–P(2)	144.7(2)
B(8)–Ir(7)–P(1)	76.5(3)	B(6)–Ir(7)–P(2)	80.4(3)
B(9)–Ir(7)–P(1)	105.5(3)	B(9)–Ir(7)–P(2)	107.3(3)
B(4)–Ir(7)–B(3)	56.5(4)		
B(6)–Ir(7)–B(3)	43.5(3)	B(8)–Ir(7)–B(4)	43.9(3)
C(10)–Ir(7)–B(3)	80.5(4)	C(10)–Ir(7)–B(4)	84.0(4)
B(8)–Ir(7)–B(3)	85.3(4)	B(6)–Ir(7)–B(4)	85.0(4)
B(9)–Ir(7)–B(3)	69.4(4)	B(9)–Ir(7)–B(4)	69.1(4)
C(10)–Ir(7)–B(6)	117.1(4)	C(10)–Ir(7)–B(8)	123.2(4)
B(8)–Ir(7)–B(6)	84.7(4)		
B(9)–Ir(7)–B(6)	44.8(3)	B(9)–Ir(7)–B(8)	44.0(2)
C(10)–Ir(7)–B(9)	147.4(3)		

(*ii*) At boron and carbon

Ir(7)–B(3)–C(1)	102.7(5)	Ir(7)–B(3)–B(2)	99.5(6)
B(2)–B(3)–C(1)	57.4(6)	Ir(7)–B(3)–B(6)	61.8(4)
B(6)–B(3)–C(1)	108.7(7)	B(2)–B(3)–B(6)	58.3(6)
C(1)–B(4)–Ir(7)	103.4(5)	B(5)–B(4)–Ir(7)	99.3(5)
B(5)–B(4)–C(1)	57.7(5)	B(8)–B(4)–Ir(7)	61.6(4)
B(8)–B(4)–C(1)	108.9(7)	B(8)–B(4)–B(5)	58.0(5)
B(3)–C(1)–B(2)	66.9(6)	B(4)–C(1)–B(2)	114.0(7)
B(4)–C(1)–B(3)	89.9(6)	B(5)–C(1)–B(2)	69.0(6)
B(5)–C(1)–B(3)	113.7(7)	B(5)–C(1)–B(4)	66.5(6)

for the *isonido* and *isocloso* species are also gathered in Table 6. Fig. 4 plots *b versus* θ for this set of compounds, and it can be seen that there are several points along the continuum from nine-vertex *closo* to square-faced '*isonido*' geometry, but that there is a gap between *isonido* and *isocloso*. A similar *isonido*–*isocloso* gap has been noted in the ten-vertex continuum,[6] and there, as here, it is not yet certain whether this merely reflects the chemistry that happens to have been investigated so far, or whether there is a catastrophic flip from *isonido* to *closo* as the fold angle θ passes a critical value.

Geometrically the *isonido* nine-vertex cluster is derived from the ten-vertex *isocloso* cluster by the removal of a vertex of cluster connectivity four. This derivation parallels that of the ten-vertex *isonido* cluster which results from the eleven-vertex *isocloso* cluster also by the removal of a vertex of cluster connectivity four. Here it is noted that the eleven-vertex C_{2v} closed structure is unique in that the shape is reproduced by one d.s.d. operation,[15] so in this sense the eleven-vertex *closo* and *isocloso* structures have the same gross geometry.

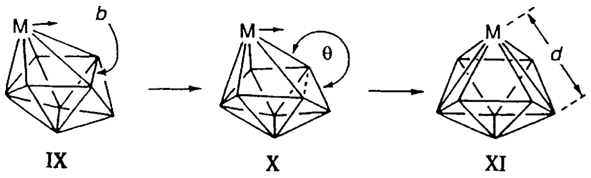

Scheme 1

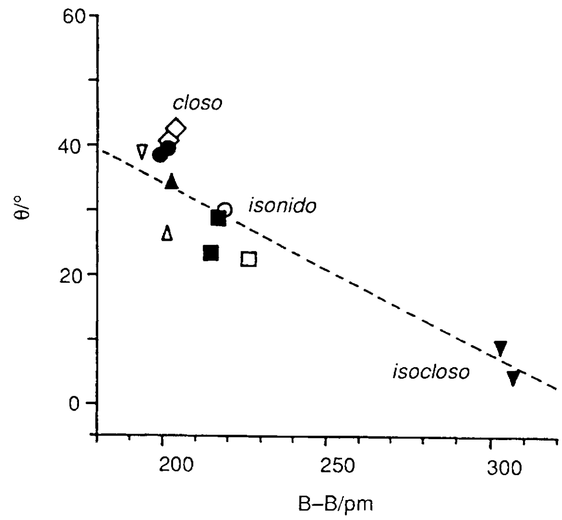

Fig. 4 The nine-vertex *closo*–*isonido*–*isocloso* structural continuum. Plot of the diamond-square–diamond diagonal distance *b* (as defined in Scheme 1) *versus* the cluster fold angle θ. It is not yet certain whether the lack of examples between *isonido* and *isocloso* merely reflects the lack of research in the area, or whether there is a 'catastrophic flip' from *isonido* to *isocloso* as the parameters pass critical values (compare ref. 6).

These perceptions adduce to a conclusion that these *isocloso* and *isonido* types of structure, and structural continua among these and the classical *closo*, can be quite general in polyhedral boron-containing chemistry, and it is useful briefly to develop this context. For example, it is becoming apparent that they feature in eleven- and twelve- and possibly also eight-vertex systems, as well as in the nine-vertex systems dealt with in this paper and in the ten-vertex systems[5,6] mentioned in the previous two paragraphs.

In eleven-vertex closed cluster systems an extended structural continuum *within* the constraints of the formal *closo* C_{2v} symmetry has been established recently.[16] Alternatively, and more of a parallel to the results in this present work, formally *closo* eleven-vertex systems such as [1-H-1,1-$(PPh_3)_2$-1,2,4-$IrC_2B_8H_{10}$][17] can exhibit opening to quadrilaterally faced '*isonido*'.[16,17] Here species such as [$(C_5Me_5)_2HRhIrB_9H_{10}$],[18] the eleven-vertex {Rh_2B_9} subcluster of [$(C_5Me_5)RhB_9$-$(SMe_2)H_{10}RhB_9H_7(SMe_2)$],[19] and then [$(PMe_3)_2H(PPh_3)$-$(Ph_2PC_6H_4)PtIrB_9H_{10}$][20] exhibit successive steps along a continuum from *isonido* to pentagonally open-faced classical *nido*. A compound such as [2-(C_6Me_6)-'*nido*'-2,8,10-$OsC_2B_8H_8$-Me_2-8,10],[21] still of formal *closo* electron count, thence demonstrates further opening to hexagonally open-faced eleven-vertex '*isoarachno*' geometry. These eleven-vertex *isonido* and '*isoarachno*' geometries both derive from a twelve-vertex *isocloso* icosahedron (see below) by the removal of either a four- or a six-connected vertex respectively. The '*isoarachno*' opening

Table 6 Diamond–square–diamond diagonals and fold angles in the nine-vertex *closo–isonido–isocloso* sequence

Compound	BB diagonal *b*/pm	Other diagonal *d*/pm	Fold angle θ/°	Ref.
$[B_9H_9]^{2-}$	193(2)	287(2)	39.6(8)	9
$[1,6\text{-}Me_2\text{-}1,6\text{-}C_2B_7H_7]$	201.4(12)	291.4(12)	39.6(8)	10
	199.7(12)	290.7(13)	39.3(8)	
$[1,5\text{-}(SMe_2)_2B_9H_7]$	202.9(11)	278.1(11)	42.6(7)	11
	201.9(12)	285.2(12)	41.4(7)	
$[(C_5H_5)CoCB_7H_8]^-$	202.4(14)	388.5(9)	26.6(10)	12
$[(PEt_3)_2HCoC_2B_6H_8]$[a]	203.1	308.4	34.9	13
$[(CO)_3MnC_2B_6H_8]^-$	212.2(7)	334.4(7)	23.9(5)	14
$[(CO)(PPh_3)HIrCB_7H_7(PPh_3)]$	218.7(9)	320.0(6)	29.4(3)	This work
$[(CO)(PPh_3)_2IrCB_7H_8]$	219.0(14)	321.2(9)	30.3(8)	1
$[(CO)(PPh_3)_2IrCB_7H_8]$[b]	226.2(11)	316.3(7)	25.9(4)	This work
$[(PMe_3)_2HIrB_8H_7Cl]$	307(2)	231.5(9)	4.5(11)	7
	304(2)	230.7(10)	8.8(11)	

[a] No e.s.d.s available for this structure. [b] As CH_2Cl_2 disolvate.

is reminiscent of the anomalous opening observed in the ten-vertex formally *nido* species $[1\text{-}(C_6Me_6)\text{-}1\text{-}RuB_9H_{13}]$,[22] of which the basic cluster structure derives from the removal of adjacent six- and five-connected vertices from the twelve-vertex *isocloso* shape.

Fewer results are available in twelve-vertex boron-containing cluster chemistry, but corresponding *isocloso* and *isonido* behaviour is already apparent from experimental results. Thus $[\{(Et_3P)_2Pt\}(\mu\text{-}CO)_2WC_2B_9H_8Me_2(CH_2C_6H_4Me\text{-}4)]$[23] exhibits an '*isocloso*' icosahedral structure derived from classical *closo* icosahedral by a d.s.d. process, and [3-(C_5Me_5)-'*closo*'-3,1,2-$RhC_2B_9H_9Ph_2$-1,2][24] exhibits a quadrilaterally open-faced '*isonido*' structure intermediate between these two extremes. Here also $[(PMe_2Ph)_2Pt_2B_{10}H_{10}]$ of classical *closo* geometry exists in equilibrium with its (reasonably presumed) *isocloso* isomer,[25] emphasising the energetic similarities of the two cluster types when the cluster constituents are apposite. As mentioned above, the twelve-vertex *isocloso* cluster is the parent for *isonido* and *isoarachno* shapes of lower vertex number by the removal of vertices. Analogously, the twelve-vertex *isonido* structure can be generated by the removal of a vertex of connectivity four from typical thirteen-vertex closed geometries such as that of $[(C_5H_5)CoC_2B_{10}H_{12}]$,[26] in which the thirteen-vertex *closo* cluster exhibits the four- and six-connected vertices that also typify the *isocloso* cluster shapes that have fewer vertices. Of additional interest in the present context is that it also exhibits a partial d.s.d. opening in the solid state, and a cluster fluxionality in solution.[26]

In the general case this type of fluxional behaviour of *closo*-type cluster compounds is significant as it implies open *nido* or *isonido* structures of very similar energy.[27] In eight-vertex chemistry [*closo*-$B_8H_8]^{2-}$, [*closo*-$CB_7H_8]^-$, [*closo*-$CB_7H_7I]^-$ and [*closo*-$CB_7H_6I_2]^-$ all have classical dodecahedral clusters in the solid state in salts examined so far,[28] but they are very fluxional in solution, implying open-face isomers of very similar energies. This in turn implies that suitable cluster substituents or constituents will readily stabilise open clusters in this '*closo*' eight-vertex system also. It may be that relatively simple modifications, such as protonation,[29] or crystallisation with a small polarising counter cation can achieve this in these anionic eight-vertex systems.

Conclusion

The experimental results in this paper together with those just summarised show that many classically *closo* species in twelve-, eleven-, ten-, nine- and also probably eight-vertex boron cluster chemistry exhibit partial opening towards square-faced *isonido* structures, and with suitable cluster constituents and substituents a complete opening can be induced to generate stable and isolatable *isonido* species. These openings may be induced sterically, electronically, or sometimes by crystal-packing forces if the energy differences are small.[27] Completion of this d.s.d. process gives *isocloso* structures, of which examples are also isolatable. Geometrical removal of vertices of cluster connectivity four from *n*-vertex *isocloso* geometries generates the $(n - 1)$-vertex *isonido* geometries, and removal of two adjacent vertices from *isocloso* appears to generate $(n - 2)$-vertex *isoarachno* geometries, although experimental results in this last area are still sparse. There appear to be emerging parallels here to the vertex-removal concepts involved in the classical Williams–Wade–Rudolph[3,4,30] structural patterns, and for these new '*iso*' geometries it is now possible[27] to start the construction of a general *isocloso–isonido–isoarachno* structural relationship (Fig. 5), analogous to the classical *closo–nido–arachno* one commonly depicted[30] in the general literature. A general recognition, and a further experimental delineation, of these various structural continua, and a general recognition of the new structural symmetries revealed, should form the basis of useful extensions to the classical Williams–Wade[3,4,30] cluster-structure/electron-counting formalism, and the basis of rigorous molecular-orbital approaches to account for them.

Experimental

General.—The reactions were carried out under dry dinitrogen though subsequent operations, *e.g.* analytical and preparative thin-layer chromatography (TLC), were carried out in air. The starting compound [7-(CO)-7,7-$(PPh_3)_2$-7,1-$IrCB_7H_8$] **1** was prepared from $[IrCl(CO)(PPh_3)_2]$ and [*closo*-$CB_7H_8]^-$ by the literature method.[1] Chloroform was distilled from P_4O_{10}, and dichloromethane from CaH_2, prior to use. The pentane and dichloromethane used for high-pressure liquid chromatography (HPLC) were of 'HPLC grade' and used as received. Other substances were of reagent or analytical grade and were used as purchased. All evaporations of solvents were carried out using standard rotary evaporation techniques. Preparative TLC was carried out using silica gel G (Fluka, type GF 254) as the stationary phase on plates of dimensions 200 × 200 × 1 mm, made on glass formers from aqueous slurries followed by drying in air at 80 °C. The purity of individual chromatographic fractions was checked by analytical TLC on Silufol (Kavalier, silica gel G on aluminium foil) (detection using UV and/or aqueous $AgNO_3$ spray). Preparative HPLC was performed using a Lichrosorb Si60 7 μm silica gel column (260 × 16 mm; N_t *ca.* 4200 theoretical plates); mobile phase CH_2Cl_2–C_5H_{12} (3 : 7 v/v); flow rate 15 $cm^3\ min^{-1}$; sensitivity 8/10; sample concentration 2.4×10^{-3} cm^{-3}; UV detection at 240 nm.

Physical Measurements.—Proton (^1H), boron (^{11}B) and phosphorus (^{31}P) NMR spectroscopy was carried out at 2.35

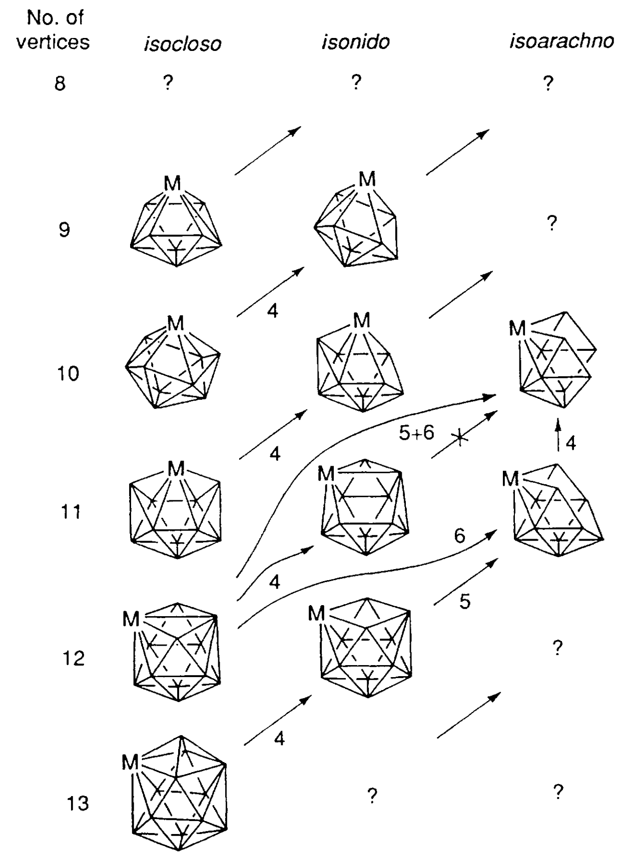

Fig. 5 Schematic of an emerging pattern of structural relationships among the *isocloso*, *isonido* and *isoarachno* boron-containing cluster systems (compare the classical *closo*/*nido*/*arachno* pattern, *e.g.* ref. 30). The *isocloso* system is generated from the classical *closo* by a d.s.d. process; removal of a vertex of low connectivity from an *n*-vertex *isocloso* generates the ($n - 1$)-vertex '*isonido*' geometry, and removal of two adjacent vertices generates the ($n - 2$)-vertex '*isoarachno*' geometry. The numbers by the arrows indicate the cluster connectivities of the removed vertices. Experimental results appropriate for the *isoarachno* column are as yet sparse. The eight-vertex area is as yet unexamined for '*iso*' behaviour, although the very ready cluster fluxionality of some eight-vertex *closo* anions suggests that the appropriate alternative cluster structures are inherently isolatable. The *iso* cluster structures are characterised by one or more vertices which have high cluster connectivities, and in examples characterised so far one or more of these is generally a transition-metal centre, designated as M in this Figure

and 9.4 T on commercially available JEOL FX-100 and Bruker AM-400 instruments respectively. The ^{1}H-{^{11}B(selective)} NMR experiments were performed essentially as described previously.[31] Chemical shifts δ are given in ppm to high frequency (low field) of Ξ = 32.083 971 [nominally $BF_3(OEt_2)$ in $CDCl_3$] for ^{11}B (quoted ±0.5 ppm), 40.480 730 (nominally 85% H_3PO_4) for ^{31}P (quoted ±0.5 ppm) and 100 MHz ($SiMe_4$) for ^{1}H (quoted ±0.05 ppm), Ξ being defined as in ref. 32. Solvent resonances were used as internal secondary standards. Coupling constants $^{1}J(^{11}B-^{1}H)$ could not be defined because of the general broadness of the ^{11}B resonances which arises from the relatively large molecular size of the compounds under study.

Syntheses.—Thermal rearrangement of [7-(CO)-7,7-$(PPh_3)_2$-7,1-$IrCB_7H_8$] **1**. A typical procedure was as follows. Compound **1** (11 mg, 13.1 μmol) was heated at 250 °C for *ca.* 10 min *in vacuo*. The resulting mixture was then allowed to cool spontaneously to ambient temperature, dissolved in dichloromethane (*ca.* 2 cm^3), and subjected to preparative TLC using chloroform as the liquid phase. The main orange-yellow band [R_f(preparative) 0.9, (analytical) 0.61] was collected to give 10.7 mg of an approximately 1 : 1 : 3 mixture of compounds **1**–**3** respectively, as assessed from integrated ^{31}P and ^{11}B NMR measurements. The mixture was separated *via* repeated preparative HPLC experiments, using CH_2Cl_2–C_5H_{12} (3 : 7 v/v) as the liquid phase. Evaporation to dryness of the three pure chromatographic fractions ultimately obtained ($k' = 3.50$, 3.73 and 4.40, k' being defined as in ref. 33) then gave orange compounds which were identified by NMR spectroscopy and X-ray diffraction analysis as **1** (1.1 mg, 10% recovery), **2** (2.8 mg, 26%) and **3** (5.3 mg, 48%), respectively. The crystal of compound **3** for crystallographic measurements was grown from a dichloromethane solution that had been overlayered by an equal volume of hexane.

X-Ray Crystallography.—All crystallographic measurements were made at 200 K on a Stoe STADI4 diffractometer operating in the ω–θ scan mode and using graphite-monochromated Mo-Kα radiation (λ = 71.069 pm), with scan speeds 1.5–8.0° min^{-1} and scan widths of 1.05° + α-doublet splitting. The structures of both **1** and **3** were solved using standard heavy-atom methods and refined by full-matrix least-squares refinement using SHELX 76.[34] All non-hydrogen atoms for both compounds were refined with anisotropic thermal parameters, with the exception of the chlorine and carbon atoms of the disordered CH_2Cl_2 solvent molecules (two molecules for **1** and one for **3**) which were refined with isotropic thermal parameters and a 50 : 50 occupancy ratio over the two disordered orientations in each case. Each phenyl group was treated as a rigid body with idealised hexagonal symmetry (C–C 139.5 pm) with phenyl hydrogen atoms included in calculated positions (C–H 96 pm), and refined with an overall isotropic thermal parameter. Borane cluster hydrogen atoms were located in Fourier difference maps and freely refined with individual isotropic thermal parameters. Both data sets were corrected for absorption empirically using azimuthal ψ scans. The weighting scheme $w = [\sigma^2(F_o) + g(F_o)^2]^{-1}$ was used with $g = 0.0003$ for **1** and 0.0004 for **3**. Non-hydrogen and cluster hydrogen fractional atomic coordinates for **1** and **3** are in Tables 7 and 8 respectively.

Crystal data. **1** [bis(dichloromethane) solvate], $C_{38}H_{38}B_7IrOP_2{\cdot}2CH_2Cl_2$, $M = 1010.4$ (includes solvent molecules), dimensions 0.55 × 0.3 × 0.15 mm, monoclinic, space group $P2_1/n$, $a = 1394.33(10)$, $b = 1276.81(13)$, $c = 2393.5(2)$ pm, $\beta = 94.163(9)°$, $U = 4.2498(6)$ nm^3, $Z = 4$, $D_c = 1.58$ Mg m^{-3}, $\mu = 21.48$ cm^{-1}, $F(000) = 3135.97$, $T = 200$ K, $R(R_g) = 0.0351$ (0.0384) for the refinement of 5991 absorption-corrected reflections with $I > 2.0\sigma(I)$ and $4.0 < 2\theta < 50.0°$.

Compound **3** (dichloromethane solvate), $C_{38}H_{38}B_7IrOP_2{\cdot}CH_2Cl_2$, $M = 925.90$ (includes solvent molecule), dimensions 0.38 × 0.35 × 0.32 mm, triclinic, space group $P\bar{1}$, $a = 1150.39(11)$, $b = 1177.08(13)$, $c = 1498.3(2)$ pm, $\alpha = 88.192(9)$, $\beta = 89.506(8)$, $\gamma = 80.720(9)°$, $U = 2.0013(4)$ nm^3, $Z = 2$, $D_c = 1.54$ Mg m^{-3}, $\mu = 34.23$ cm^{-1}, $F(000) = 915.96$, $T = 200$ K, $R(R_g) = 0.0299$ (0.0311) for the refinement of 5864 absorption-corrected reflections with $I > 2.0\sigma(I)$ and $4.0 < 2\theta < 50.0°$.

Additional material available from the Cambridge Crystallographic Data Centre comprises thermal parameters and remaining bond lengths and angles.

Acknowledgements

Contribution no. 34 from the Řež–Leeds Anglo–Czech Polyhedral Collaboration (ACPC). We thank the SERC (grants nos. GR/F/43215 and GR/F/78323), The Czech Academy of Sciences (grant no. 43204), Borax Research Ltd., and the Royal Society for support, Drs. D. M. Wagnerová, T. S. Griffin and R. A. Walker for helpful co-operation, and Dr. K. Nestor for useful discussions.

Table 7 Non-hydrogen (× 10^4) and cluster hydrogen (× 10^3) fractional coordinates for compound **3**

Atom	x	y	z	Atom	x	y	z
Ir(7)	1686.1(2)	2053.3(2)	2338.9(1)	C(223)	−976(3)	3889(3)	4927(2)
P(1)	2950.4(11)	1165.3(11)	3447.2(8)	C(224)	−1874(3)	4777(3)	5158(2)
P(2)	−686.8(10)	4411.3(10)	2215.7(8)	C(225)	−2397(3)	5558(3)	4503(2)
C(111)	4267(2)	1852(3)	3546(2)	C(226)	−2023(3)	5452(3)	3617(2)
C(112)	4105(2)	3039(3)	3657(2)	C(231)	−2048(2)	4935(3)	1624(2)
C(113)	5079(2)	3596(3)	3749(2)	C(232)	−2215(2)	5970(3)	1127(2)
C(114)	6214(2)	2965(3)	3729(2)	C(233)	−3298(2)	6363(3)	720(2)
C(115)	6376(2)	1777(3)	3618(2)	C(234)	−4213(2)	5720(3)	810(2)
C(116)	5403(2)	1221(3)	3526(2)	C(235)	−4046(2)	4686(3)	1308(2)
C(121)	2360(3)	1215(3)	4591(2)	C(236)	−2963(2)	4293(3)	1715(2)
C(122)	3079(3)	1344(3)	5314(2)	C(10)	2913(5)	2661(6)	1768(4)
C(123)	2624(3)	1347(3)	6181(2)	O(10)	3627(4)	3043(5)	1387(3)
C(124)	1451(3)	1221(3)	6324(2)	C(1)	279(5)	1207(5)	720(4)
C(125)	733(3)	1092(3)	5601(2)	B(2)	−712(6)	2027(5)	1275(4)
C(126)	1187(3)	1089(3)	4734(2)	B(3)	681(6)	2402(5)	954(4)
C(131)	3554(3)	−353(2)	3304(2)	B(4)	1385(6)	605(5)	1301(4)
C(132)	3586(3)	−1176(2)	3998(2)	B(5)	−96(6)	483(5)	1595(4)
C(133)	4056(3)	−2323(2)	3850(2)	B(6)	−20(5)	2881(5)	1924(4)
C(134)	4494(3)	−2648(2)	3009(2)	B(8)	950(2)	489(5)	2392(4)
C(135)	4462(3)	−1825(2)	2315(2)	B(9)	−240(5)	1628(5)	2488(4)
C(136)	3992(3)	−678(2)	2462(2)	H(1)	15(6)	105(6)	7(5)
C(211)	304(3)	5424(3)	1960(2)	H(2)	−162(5)	233(5)	102(4)
C(212)	900(3)	5352(3)	1144(2)	H(3)	103(5)	289(5)	39(4)
C(213)	1626(3)	6155(3)	907(2)	H(4)	214(5)	−9(5)	102(4)
C(214)	1756(3)	7030(3)	1487(2)	H(5)	−54(5)	−23(5)	153(4)
C(215)	1160(3)	7102(3)	2303(2)	H(7)	152(5)	312(5)	283(4)
C(216)	434(3)	6299(3)	2539(2)	H(8)	117(4)	−19(4)	288(4)
C(221)	−1125(3)	4564(3)	3386(2)	H(9)	−85(4)	165(4)	307(3)
C(222)	−602(3)	3783(3)	4041(2)				

Table 8 Non-hydrogen (× 10^4) and cluster hydrogen (× 10^3) fractional coordinates for compound **1**

Atom	x	y	z	Atom	x	y	z
Ir(7)	3099.60(10)	1733.2(2)	1321.60(10)	C(223)	1670(3)	5535(2)	1112(2)
P(1)	4489.4(10)	2850.8(12)	1471.8(6)	C(224)	1199(3)	6003(2)	642(2)
P(2)	2323.8(10)	2599.6(11)	513.0(6)	C(225)	1093(3)	5457(2)	136(2)
C(111)	5480(2)	2688(3)	1016.8(14)	C(226)	1457(3)	4444(2)	100(2)
C(112)	5442(2)	1926(3)	598.1(14)	C(231)	1120(2)	2073(3)	305(2)
C(113)	6179(2)	1857(3)	235.3(14)	C(232)	878(2)	1575(3)	−204(2)
C(114)	6953(2)	2551(3)	291.2(14)	C(233)	−58(2)	1215(3)	−329(2)
C(115)	6991(2)	3313(3)	710.0(14)	C(234)	−752(2)	1353(3)	57(2)
C(116)	6254(2)	3381(3)	1072.8(14)	C(235)	−510(2)	1851(3)	566(2)
C(121)	4305(3)	4271(2)	1379(2)	C(236)	426(2)	2211(3)	691(2)
C(122)	4261(3)	4642(2)	830(2)	C(10)	2322(4)	2436(5)	1811(3)
C(123)	4088(3)	5701(2)	721(2)	O(10)	1817(3)	2732(4)	2130(2)
C(124)	3959(3)	6390(2)	1162(2)	C(1)	2699(5)	−416(5)	1919(3)
C(125)	4003(3)	6019(2)	1711(2)	B(2)	2677(6)	−740(6)	1258(4)
C(126)	4176(3)	4960(2)	1820(2)	B(3)	2030(6)	334(6)	1522(4)
C(131)	5036(3)	2743(3)	2192.4(12)	B(4)	3388(6)	555(6)	2086(3)
C(132)	4439(3)	2869(3)	2630.8(12)	B(5)	3789(6)	−550(6)	1717(3)
C(133)	4819(3)	2788(3)	3184.5(12)	B(6)	2473(5)	371(5)	875(3)
C(134)	5795(3)	2581(3)	3299.9(12)	B(8)	4240(5)	656(5)	1607(3)
C(135)	6392(3)	2455(3)	2861.5(12)	B(9)	3698(5)	105(5)	1011(3)
C(136)	6012(3)	2536(3)	2307.8(12)	H(1)	246(5)	−88(6)	223(3)
C(211)	2999(3)	2536(3)	−124.5(14)	H(2)	254(5)	−160(5)	107(3)
C(212)	3279(3)	1552(3)	−306.8(14)	H(3)	120(5)	50(6)	153(3)
C(213)	3730(3)	1456(3)	−805.6(14)	H(4)	356(4)	84(5)	253(2)
C(214)	3903(3)	2345(3)	−1122.0(14)	H(5)	408(6)	−126(7)	186(3)
C(215)	3624(3)	3330(3)	−939.7(14)	H(6)	211(4)	39(5)	46(3)
C(216)	3172(3)	3425(3)	−440.9(14)	H(8)	503(5)	91(6)	171(3)
C(221)	1928(3)	3976(2)	570(2)	H(9)	413(4)	−10(4)	67(2)
C(222)	2034(3)	4521(2)	1076(2)				

References

1 B. Štíbr, J. D. Kennedy, M. Thornton-Pett, E. Drdáková, T. Jelínek and J. Plešek, *Collect. Czech. Chem. Commun.*, 1992, **57**, 1439.

2 C. K. Johnson, ORTEP, Report ORNL 5138, Oak Ridge National Laboratory, Oak Ridge, TN, 1976.

3 R. E. Williams, *Inorg. Chem.*, 1971, **10**, 210; *Adv. Inorg. Chem. Radiochem.*, 1978, **18**, 64.

4 K. Wade, *Chem. Commun.*, 1971, 792; *Adv. Inorg. Chem. Radiochem.*, 1978, **18**, 1.

5 K. Nestor, B. Štíbr, J. D. Kennedy, M. Thornton-Pett and T. Jelínek, *Collect. Czech. Chem. Commun.*, 1992, **57**, 1262.

6 J. Bould, J. D. Kennedy and M. Thornton-Pett, *J. Chem. Soc., Dalton Trans.*, 1992, 563.

7 J. Bould, J. E. Crook, N. N. Greenwood, J. D. Kennedy and W. S. McDonald, *J. Chem. Soc., Chem. Commun.*, 1982, 346.

8 W. N. Lipscomb, *Science (Washington, D.C.)*, 1966, **153**, 373.
9 L. Guggenberger, *Inorg. Chem.*, 1968, **7**, 2260.
10 T. K. Koetzle, F. E. Scarbrough and W. N. Lipscomb, *Inorg. Chem.*, 1968, **7**, 1076.
11 D. D. Bray, R. M. Kabbani and E. H. Wong, *Acta Crystallogr., Sect. B*, 1982, **38**, 957.
12 K. P. Callahan, C. E. Strouse, A. L. Sims and M. F. Hawthorne, *Inorg. Chem.*, 1974, **13**, 1393.
13 G. K. Barker, M. Green, M. P. Garcia, F. G. A. Stone, J.-M. Basset and A. J. Welch, *J. Chem. Soc., Chem. Commun.*, 1980, 1266.
14 F. J. Hollander, D. H. Templeton and A. Zalkin, *Inorg. Chem.*, 1973, **12**, 2262.
15 R. E. Wiersema and M. F. Hawthorne, *Inorg. Chem.*, 1973, **12**, 785.
16 J. D. Kennedy, B. Štíbr, T. Jelínek, X. L. R. Fontaine and M. Thornton-Pett, *Collect. Czech. Chem. Commun.*, 1993, **58**, 2090.
17 K. Nestor, X. L. R. Fontaine, N. N. Greenwood, J. D. Kennedy, J. Plešek, B. Štíbr and M. Thornton-Pett, *Inorg. Chem.*, 1989, **28**, 2219.
18 K. Nestor, X. L. R. Fontaine, N. N. Greenwood, J. D. Kennedy and M. Thornton-Pett, *J. Chem. Soc., Chem. Commun.*, 1989, 455.
19 E. J. Ditzel, X. L. R. Fontaine, N. N. Greenwood, J. D. Kennedy and M. Thornton-Pett, *J. Chem. Soc., Chem. Commun.*, 1989, 1262.
20 J. Bould, J. E. Crook, J. D. Kennedy and M. Thornton-Pett, *Inorg. Chim. Acta*, 1993, **203**, 193.
21 M. Bown, X. L. R. Fontaine, N. N. Greenwood, J. D. Kennedy and M. Thornton-Pett, *J. Chem. Soc., Chem. Commun.*, 1987, 1650.
22 M. Bown, X. L. R. Fontaine, N. N. Greenwood, J. D. Kennedy and P. MacKinnon, *J. Chem. Soc., Chem. Commun.*, 1987, 817.
23 M. J. Attfield, J. A. K. Howard, A. N. de Jelfs, C. M. Nunn and F. G. A. Stone, *J. Chem. Soc., Dalton Trans.*, 1987, 2219; see also, N. Carr, D. F. Mullica, E. L. Sappenfield and F. G. A. Stone, *Organometallics*, 1992, **11**, 3697.
24 Z. G. Lewis and A. J. Welch, *J. Organomet. Chem.*, 1992, **430**, C45.
25 Y. M. McKinnes and M. Thornton-Pett, *Abstracts Sixth International Meeting on Boron Chemistry (IMEBORON VI), Bechyně, June 1987*, p. 55, Abstract no., CA 16; J. D. Kennedy, Y. M. McInnes and M. Thornton-Pett, 1994, to be submitted.
26 D. F. Dustin, G. B. Dunks and M. F. Hawthorne, *J. Am. Chem. Soc.*, 1973, **95**, 1109; M. R. Churchill and B. G. De Boer, *Inorg. Chem.*, 1974, **13**, 1411.
27 J. D. Kennedy, *Abstracts Eighth International Meeting on Boron Chemistry (IMEBORON VIII), Knoxville, TN, July 1993*, p. 66, Abstract no. SA 07; J. D. Kennedy and B. Štíbr, in *Current Topics in the Chemistry of Boron*, ed. G. Kabalka, The Royal Society of Chemistry, Cambridge and London, 1994, in the press.
28 T. Jelínek, B. Štíbr, J. D. Kennedy and M. Thornton-Pett, *J. Chem. Soc., Dalton Trans.*, 1994, to be submitted.
29 M. Bühl, A. M. Mebel, O. P. Charkin and P. v. R. Schleyer, *Inorg. Chem.*, 1992, **31**, 3769; see also J. W. Bausch, G. K. Surya Prakash and R. E. Williams, *Inorg. Chem.*, 1992, **31**, 3763.
30 R. W. Rudolph and W. R. Pretzer, *Inorg. Chem.*, 1972, **11**, 1974; R. W. Rudolph, *Acc. Chem. Res.*, 1976, **9**, 446.
31 X. L. R. Fontaine and J. D. Kennedy, *J. Chem. Soc., Dalton Trans.*, 1987, 1573.
32 W. McFarlane, *Proc. R. Soc. London, Ser A*, 1968, **306**, 185.
33 Z. Plzák and B. Štíbr, *J. Chromatogr.*, 1978, **151**, 363 and refs. therein.
34 G. M. Sheldrick, SHELX 76, Program System for X-Ray Structure Determination, University of Cambridge, 1976.

Received 19*th August* 1993; *Paper* 3/05041F